A Large Dendritic Multiporphyrin Array as Artificial Light-Harvesting Antenna Captures Visible Photons and Efficiently Channels the Excitation Energy to the Focal Core

Toward Artificial Photosynthesis

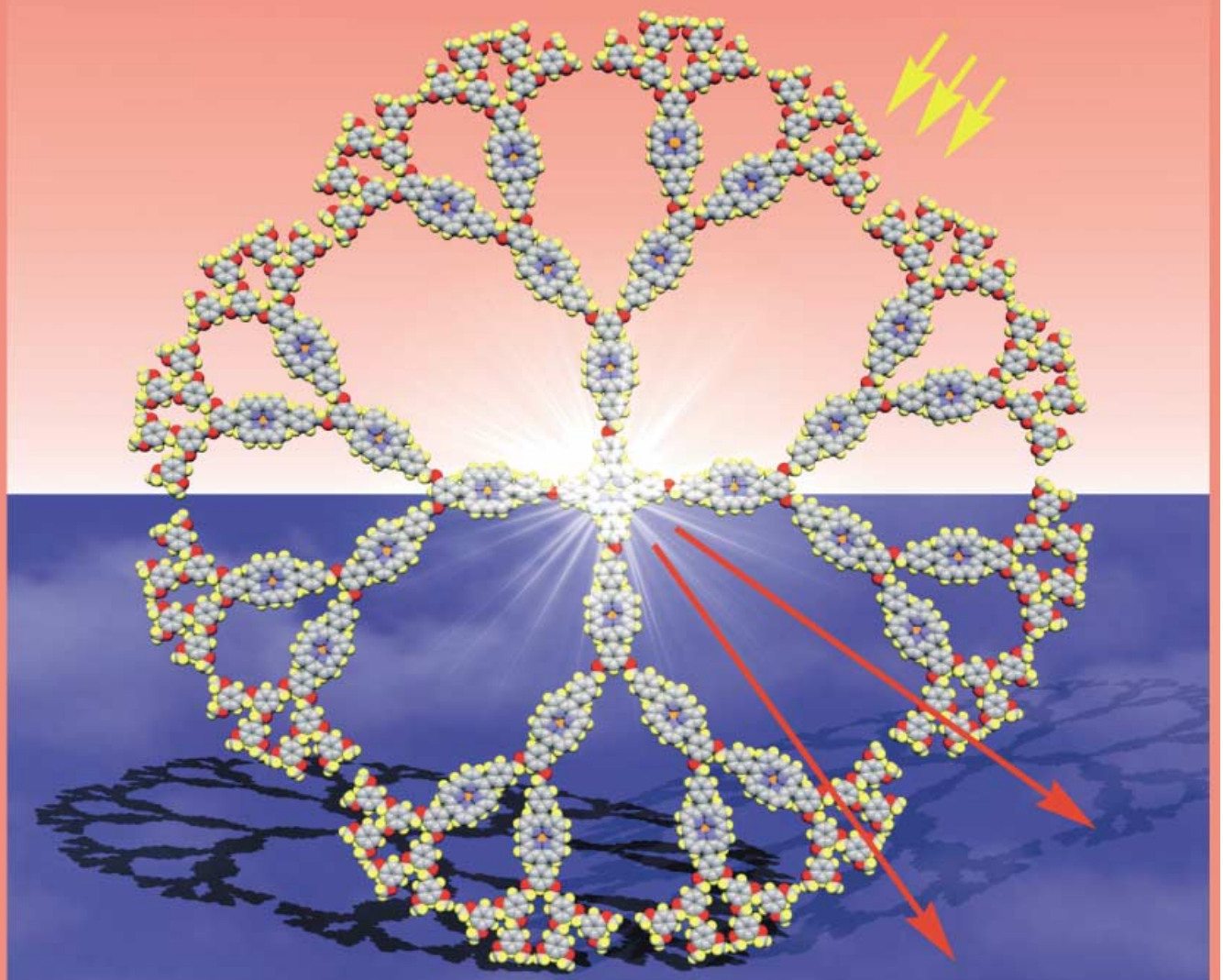

Light Harvesting with Synthetic Macromolecular Tree

For more information, see the following pages.

  0947-6539/02/0812-2667 $ 20.00+.50/0

Dendritic Multiporphyrin Arrays as Light-Harvesting Antennae: Effects of Generation Number and Morphology on Intramolecular Energy Transfer

Myung-Seok Choi,[a] Takuzo Aida,*[a] Tomoko Yamazaki,[b] and Iwao Yamazaki[b]

Abstract: A series of star- and cone-shaped dendritic multiporphyrin arrays, $(nP_{Zn})_4P_{FB}$ and $(nP_{Zn})_1P_{FB}$, respectively, that contain energy-donating dendritic zinc porphyrin (P_{Zn}) wedges of different numbers ($n = 1$, 3, and 7) of the P_{Zn} units, attached to an energy-accepting free-base porphyrin (P_{FB}) core, were synthesized by a convergent growth approach. For the cone-shaped series ($(nP_{Zn})_1P_{FB}$), the efficiency of energy transfer (Φ_{ENT}) from the photoexcited P_{Zn} units to the focal P_{FB} core, as evaluated from the fluorescence lifetimes of the P_{Zn} units, considerably decreased as the generation number increased: $(1P_{Zn})_1P_{FB}$ (86%), $(3P_{Zn})_1P_{FB}$ (66%), and $(7P_{Zn})_1P_{FB}$ (19%). In sharp contrast, the star-shaped series ($(nP_{Zn})_4P_{FB}$) all showed high Φ_{ENT} values: $(1P_{Zn})_4P_{FB}$ (87%), $(3P_{Zn})_4P_{FB}$ (80%), and $(7P_{Zn})_4P_{FB}$ (71%). Energy transfer efficiencies of $(3P_{Zn})_4$-ester-P_{FB}, $(1P_{Zn})_4$-ester-P_{FB}, and $(3P_{Zn})_1$-ester-P_{FB}, whose dendritic P_{Zn} wedges are connected by an ester linkage to the P_{FB} core, were almost comparable to those of the corresponding ether-linked versions. Fluorescence depolarization (P) studies showed much lower P values for star-shaped $(7P_{Zn})_4P_{FB}$ and $(3P_{Zn})_4P_{FB}$ than cone-shaped $(7P_{Zn})_1P_{FB}$ and $(3P_{Zn})_1P_{FB}$, respectively, indicating a highly efficient energy migration among the P_{Zn} units in the star-shaped series. Such a morphology-assisted photochemical event is probably responsible for the excellent light-harvesting activity of large $(7P_{Zn})_4P_{FB}$ molecules.

Keywords: artificial photosynthesis · dendrimers · energy conversion · light-harvesting antennae · porphyrinoids

Introduction

Artificial photosynthesis is a highly important subject, not only from the basic science point of view, but also for its possible contribution to sustainable utilization of energy resources.[1] Biological photosynthetic systems consist mainly of two functional moieties: 1) a light-absorbing antenna to efficiently capture visible photons and 2) an electron-transfer relay system to allow vectorial transfer of electrons. For these two photochemical moieties to function cooperatively, a trick is needed to allow efficient funneling of the excitation energy to the electron-transfer relay system. Since the successful structural analysis of the photosynthetic reaction center in the purple bacterium *Rhodopseudomonas viridis* in 1989,[2] much attention has been paid to molecular design to realize a vectorial transfer of electrons,[1] leading to the generation of a long-lived charge-separated state. On the other hand, model studies on artificial antenna systems have been started only quite recently.[3–5]

Artificial light-harvesting antennae require a great number of chromophore units to realize a large absorption cross section.[6] However, if these chromophore units do not cooperate with one another, the acquired light energy is scattered and the excited states decay before the energy can be channeled to the electron-transfer relay systems. Therefore, one has to consider the molecular design of an "energy funnel" to realize vectorial energy transfer to a designated point.[7] In an early stage of the research, oligomeric linear arrays[8] of chromophore units, such as porphyrin derivatives, were synthesized, in which even short-chain oligomers have difficulty in cooperative energy transport. On the other hand, in 1995, the crystal structure of the light-harvesting antenna complex (LH2) from the purple photosynthetic bacterium *Rhodopseudomonas acidophila* strain 10050 was reported which contained wheel-like arrays of bacteriochlorophyll

[a] Prof. T. Aida, M.-S. Choi
ERATO Nanospace Project
Japan Science and Technology Corporation
Department of Chemistry and Biotechnology
Graduate School of Engineering, The University of Tokyo
7-3-1 Hongo, Bunkyo-ku, Tokyo 113-8656 (Japan)
Fax: (+81) 3-5841-7310
E-mail: aida@macro.t.u-tokyo.ac.jp

[b] Dr. T. Yamazaki, Prof. I. Yamazaki
Department of Chemical Process Engineering
Graduate School of Engineering, Hokkaido University
Kita-13-Nishi-8, Kita-ku, Sapporo 060-8628 (Japan)
Fax: (+81) 11-706-6606
E-mail: yamiw@eng.hokudai.ac.jp

Supporting information for this article is available on the WWW under http://wiley-vch.de/home/chemistry/ or from the author. It contains MALDI-TOF-MS, ^{1}H NMR, and UV/Vis spectral data of star-shaped $(7P_{Zn})_4P_{FB}$, $(3P_{Zn})_4P_{FB}$, $(1P_{Zn})_4P_{FB}$, and cone-shaped $(7P_{Zn})_1P_{FB}$, $(3P_{Zn})_1P_{FB}$, $(1P_{Zn})_1P_{FB}$ (3 pages).

  0947-6539/02/0812-2668 $ 20.00+.50/0

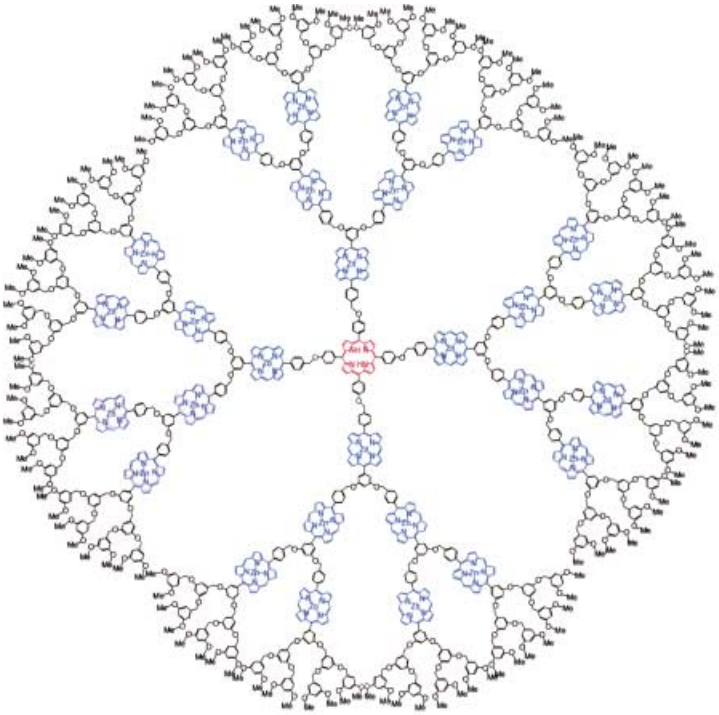

$(7P_{Zn})_4P_{FB}$

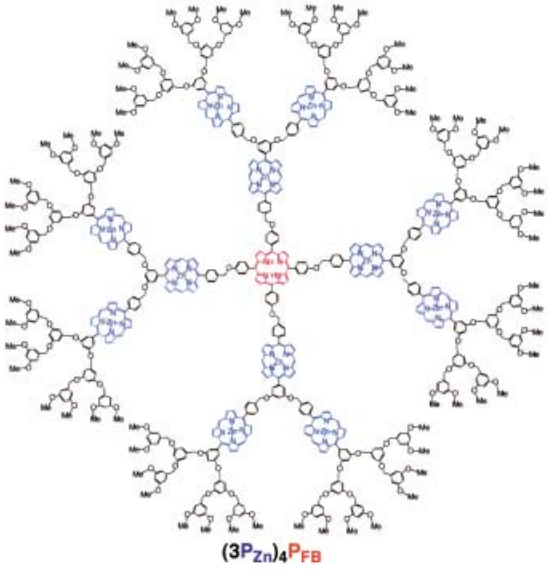

$(3P_{Zn})_4P_{FB}$

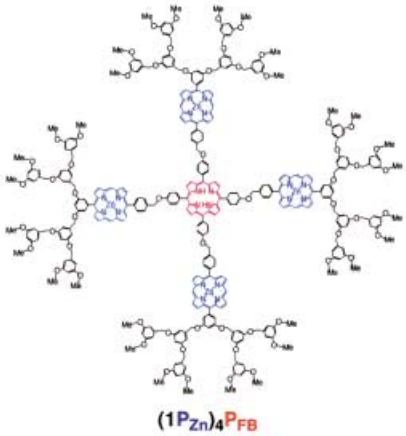

$(1P_{Zn})_4P_{FB}$

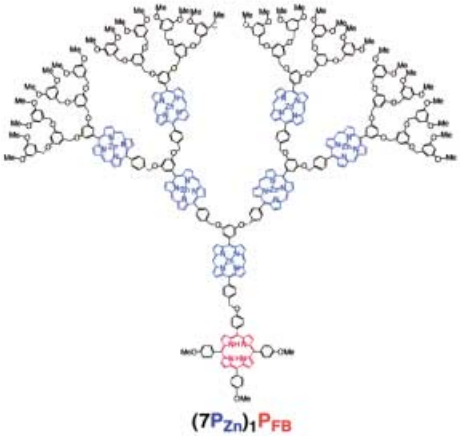

$(7P_{Zn})_1P_{FB}$

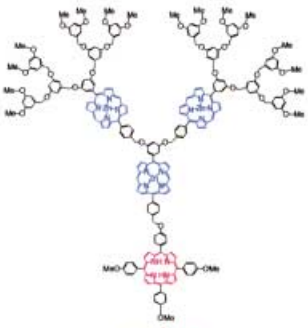

$(3P_{Zn})_1P_{FB}$

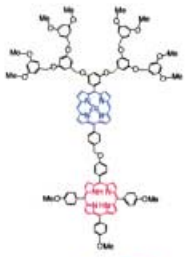

$(1P_{Zn})_1P_{FB}$

  0947-6539/02/0812-2669 $ 20.00+.50/0

units.[9] This achievement has suggested an essential importance of three-dimensional molecular architectonics of multiporphyrin arrays, to cope with both a large absorption cross section and a vectorial long-range energy transfer.

Recently, dendritic architectures have been considered as attractive scaffolds for the incorporation of a large number of light-absorbing units to allow efficient capture of dilute photons,[10, 11] and several examples of dendritic macromolecules containing porphyrin units have been synthesized.[12] In a previous communication,[13] we reported a novel star-shaped, light-harvesting multiporphyrin array $(7P_{Zn})_4P_{FB}$ consisting of four dendritic wedges of a zinc porphyrin heptamer ($7P_{Zn}$) as energy donating units, anchored by a focal free-base porphyrin (P_{FB}) core as the energy acceptor. This molecule is intended to mimic the morphology of the wheel-like chromophore array in LH2. By comparison with a cone-shaped version with a single zinc–porphyrin dendritic wedge ($(7P_{Zn})_1P_{FB}$), we found that star-shaped $(7P_{Zn})_4P_{FB}$ operates as a much more efficient energy funnel for visible photons in an analogous fashion to natural antennae.

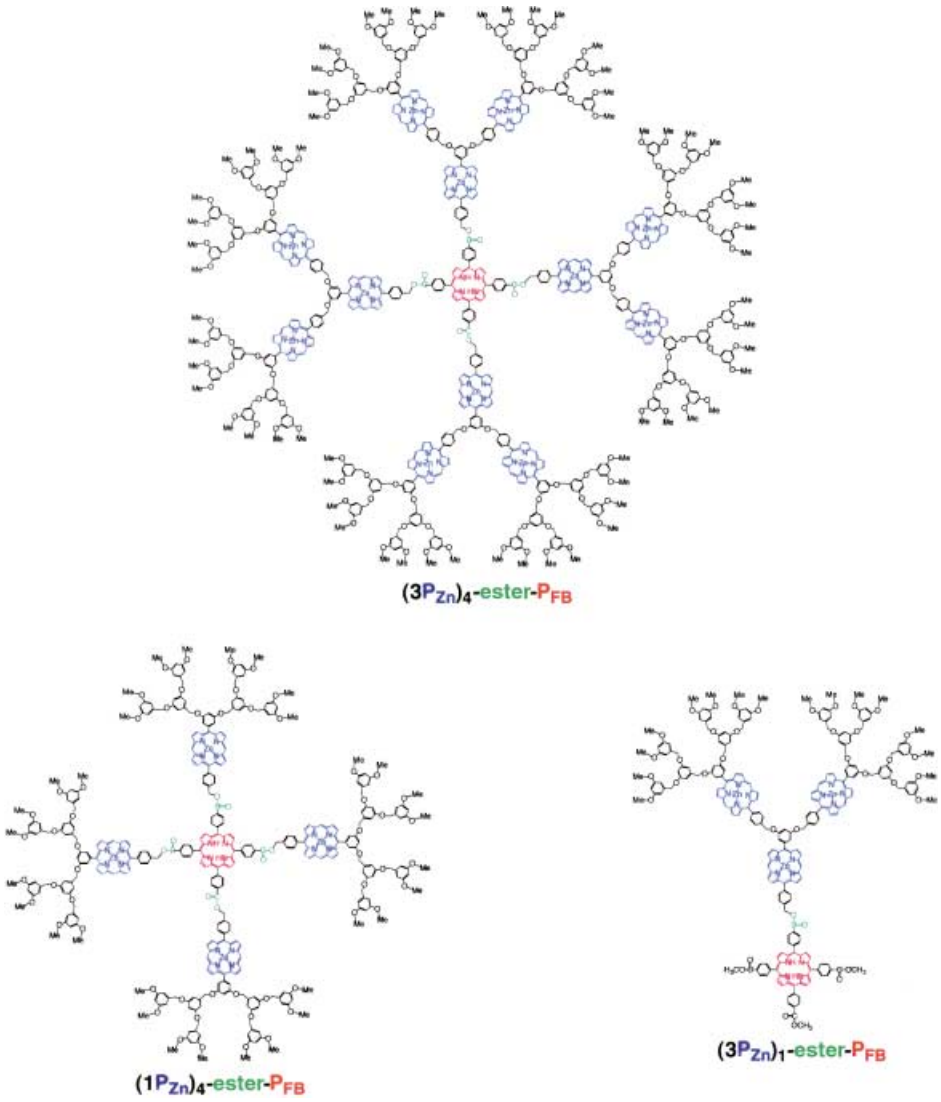

In the present paper, we report effects of generation number and morphology on intramolecular energy transfer in a series of star- and cone-shaped dendritic multiporphyrin arrays, $(nP_{Zn})_4P_{FB}$ and $(nP_{Zn})_1P_{FB}$ ($n = 1$, 3, and 7), respectively, as studied mainly by picosecond time-resolved fluorescence spectroscopies. In addition to these two series, whose dendritic wedges are linked by ether linkages to the free-base porphyrin focal core, we also synthesized some ester-linked versions of dendritic multiporphyrin arrays, $(3P_{Zn})_4$-ester-P_{FB}, $(3P_{Zn})_1$-ester-P_{FB}, and $(1P_{Zn})_4$-ester-P_{FB}, and investigated their energy transfer characteristics in comparison with the corresponding ether-linked versions.

Results and Discussion

Synthesis and identification of dendritic multiporphyrin arrays: As reported briefly in our previous communication,[13] all the dendritic multiporphyrin arrays were prepared from the fundamental building block 5-(3′,5′-dihydroxyphenyl)-15-(4′-methoxycarbonylphenyl)porphine ($(HO)_2P_{Zn}(CO_2Me)$), which was prepared by acid-catalyzed cross-condensation of 3,5-dihydroxybenzaldehyde and 4-formylbenzoic acid methyl ester with dipyrromethane, followed by oxidation. Star-shaped $(7P_{Zn})_4P_{FB}$ and cone-shaped $(7P_{Zn})_1P_{FB}$ were prepared by alkaline-mediated coupling of the corresponding dendritic zinc porphyrin containing a benzyl bromide end group $7P_{Zn}$ ($R = CH_2Br$) with 5,10,15,20-tetrakis(4′-hydroxyphenyl)porphine ($(HO)_4P_{FB}$) and 5-(4′-hydroxyphenyl)-10,15,20-tris(4′-methoxyphenyl)porphine ($(HO)_1(MeO)_3P_{FB}$), respectively (Scheme 1).[13] Likewise, lower-generation homologues, such as $(3P_{Zn})_4P_{FB}$, $(1P_{Zn})_4P_{FB}$, $(3P_{Zn})_1P_{FB}$, and $(1P_{Zn})_1P_{FB}$ were newly synthesized. On the other hand, star-shaped $(3P_{Zn})_4$-ester-P_{FB} and $(1P_{Zn})_4$-ester-P_{FB} and cone-shaped $(3P_{Zn})_1$-ester-P_{FB} were prepared from 5,10,15,20-tetrakis(4′-chlorocarbonylphenyl)porphine ($[ClC(O)]_4P_{FB}$), in place of $(HO)_4P_{FB}$, as the precursor for the free-base porphyrin focal core (Scheme 2).[14]

All the multiporphyrin arrays were isolated by recycling preparative size-exclusion chromatography (SEC) with $CHCl_3$ as eluent, and characterized by means of ^1H NMR and UV/Vis spectroscopy, together with MALDI-TOF MS.

0947-6539/02/0812-2670 $ 20.00+.50/0 *Chem. Eur. J.* **2002**, *8*, No. 12

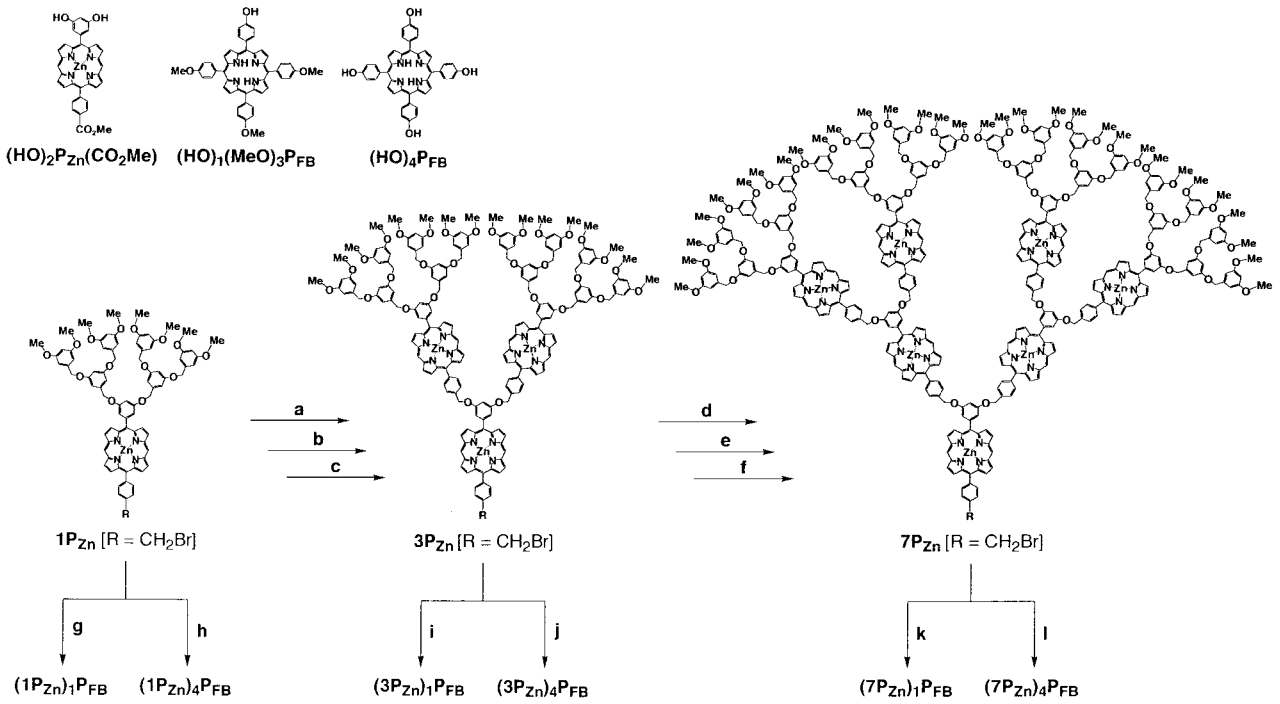

Scheme 1. Synthetic routes to star-shaped $(7P_{Zn})_4P_{FB}$, $(3P_{Zn})_4P_{FB}$, and $(1P_{Zn})_4P_{FB}$, and cone-shaped $(7P_{Zn})_1P_{FB}$, $(3P_{Zn})_1P_{FB}$, and $(1P_{Zn})_1P_{FB}$. Steps a), d) $(HO)_2P_{Zn}(CO_2Me)/K_2CO_3$/[18]crown-6, THF, 89–96%; steps b), e) $LiAlH_4$, THF, 76–99%; steps c), f) CBr_4/PPh_3, THF, 79–85%; steps g), i), k) $(HO)_1(MeO)_3P_{FB}/K_2CO_3$, NMP, 31–53%; steps h), j), l) $(HO)_4P_{FB}/K_2CO_3$, NMP, 18–62%.

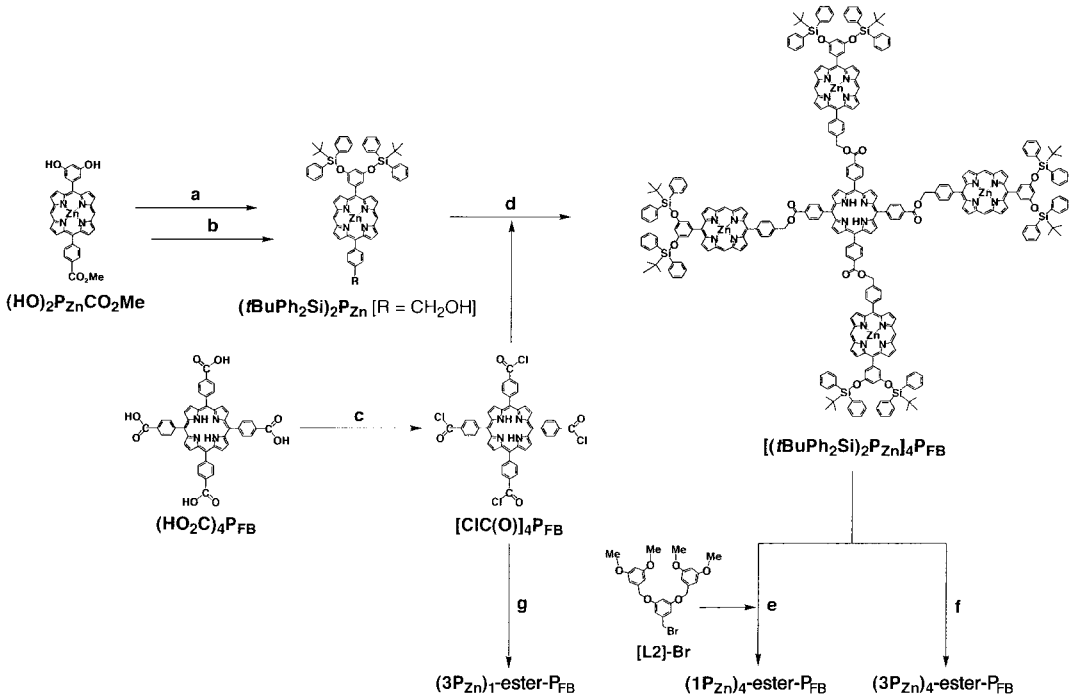

Scheme 2. Synthetic routes to $(3P_{Zn})_4$-ester-P_{FB}, $(1P_{Zn})_4$-ester-P_{FB}, and $(3P_{Zn})_1$-ester-P_{FB}. Step a) tBuPh$_2$SiCl/imidazole, DMF, 52%; step b) $LiAlH_4$, THF, 73%; step c) $(COCl)_2$, CH_2Cl_2, ~100%; step d) 4-DMAP, CH_2Cl_2, 57%; step e) KF, NMP, 60%; step f) $1P_{Zn}$ (R = CH_2Br)/KF, NMP, 16%; step g) $3P_{Zn}$ (R = CH_2OH)/4-DMAP, CH_2Cl_2; MeOH, 50%.

MALDI-TOF MS spectra of multiporphyrin arrays $(1P_{Zn})_1P_{FB}$ to $(7P_{Zn})_4P_{FB}$ showed molecular ion peaks together with multivalent ion peaks within a 0.04% deviation from the calculated values.[15] Analytical SEC of the multiporphyrin arrays produced unimodal, sharp elution peaks, where the retention time decreased as the number of the porphyrin units increased (Figure 1). The only exception is cone-shaped $(3P_{Zn})_1P_{FB}$, which eluted earlier than star-shaped $(1P_{Zn})_4P_{FB}$, despite the fact that $(3P_{Zn})_1P_{FB}$ has a lower molecular weight than $(1P_{Zn})_4P_{FB}$. Interestingly, multiporphyrin arrays with relatively high generation numbers, such as $(3P_{Zn})_4P_{FB}$ and $(7P_{Zn})_4P_{FB}$, displayed upfield shifts of some of the ^{1}H NMR

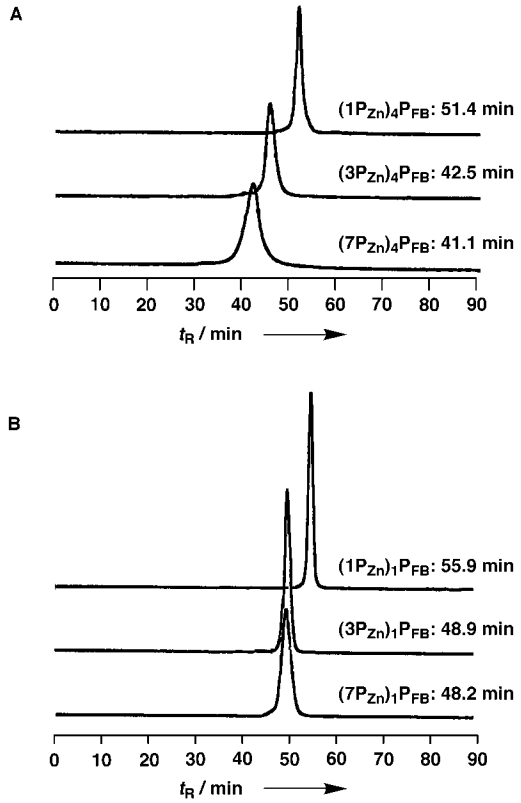

Figure 1. Size-exclusion chromatography (SEC, $CHCl_3$ as the eluent) profiles of A) star-shaped $(1P_{Zn})_4P_{FB}$, $(3P_{Zn})_4P_{FB}$, and $(7P_{Zn})_4P_{FB}$, and B) cone-shaped $(1P_{Zn})_1P_{FB}$, $(3P_{Zn})_1P_{FB}$, and $(7P_{Zn})_1P_{FB}$.

signals with significant broadening, even at an elevated temperature, such as 55 °C.[15] This indicates a rather slow conformational change of large dendritic wedges.

Electronic absorption spectroscopy: The star- and cone-shaped multiporphyrin arrays in THF at 25 °C all produced an intense Soret band with an absorption maximum at $\lambda =$ 410–415 nm together with relatively weak Q bands at $\approx$545 nm (Figure 2). The Soret absorption bands of higher generation $(7P_{Zn})_4P_{FB}$ ($\lambda_{Soret} = 415.8$ nm, FWHM = 19200 cm^{-1}) and $(3P_{Zn})_4P_{FB}$ ($\lambda_{Soret} = 415.7$ nm, FWHM = 19100 cm^{-1}) were both slightly red-shifted and broadened relative to noncovalent reference compounds prepared by mixing three monomeric porphyrins P_{Zn}^{EXT}, P_{Zn}^{INT}, and P_{FB}^{CORE} at molar ratios 16:12:1 ($\lambda_{Soret} = 414.4$ nm, FWHM = 12600 cm^{-1}) and 8:4:1 ($\lambda_{Soret} = 413.4$ nm, FWHM = 11500 cm^{-1}), respectively. On the other hand, their absorption bands in the Q-band region ($\lambda = 500-600$ nm) were hardly broadened and little shifted from those of their noncovalent references.[15] These observations indicate a weak ground-state interaction among the dendritic zinc porphyrin units.[16] $(1P_{Zn})_4P_{FB}$, the smallest homologue of the star-shaped series, showed a zinc porphyrin absorption at $\lambda = 413$ nm (for $P_{Zn}^{EXT}/P_{Zn}^{INT}/P_{FB}^{CORE} =$ 4:0:1, $\lambda_{Soret} = 413.5$ nm) with a clear shoulder at $\approx$420.9 nm, which is attributed to the free-base porphyrin core.

Similar spectral absorption characteristics were observed for the cone-shaped multiporphyrin arrays,[15] for which the Soret absorption bands of $(3P_{Zn})_1P_{FB}$ ($\lambda_{Soret} = 416.5$ nm, FWHM = 18600 cm^{-1}) and $(7P_{Zn})_1P_{FB}$ ($\lambda_{Soret} = 416.7$ nm, FWHM = 18500 cm^{-1}) were rather broad and red-shifted relative to those of their noncovalent references; $P_{Zn}^{EXT}/P_{Zn}^{INT}/P_{FB}^{CORE} = 2:1:1$ ($\lambda_{Soret} = 413.5$ nm, FWHM = 12300 cm^{-1}) and 4:3:1 ($\lambda_{Soret} = 413.3$ nm, FWHM = 11200 cm^{-1}), respectively. On the other hand, the Soret absorption band of the smallest $(1P_{Zn})_1P_{FB}$ ($\lambda_{Soret} = 413.7$, shoulder at 420.4 nm) was blue-shifted relative to that of its noncovalent reference ($\lambda_{Soret} =$ 414.9 nm for $P_{Zn}^{EXT}/P_{Zn}^{INT}/P_{FB}^{CORE} = 1:0:1$).

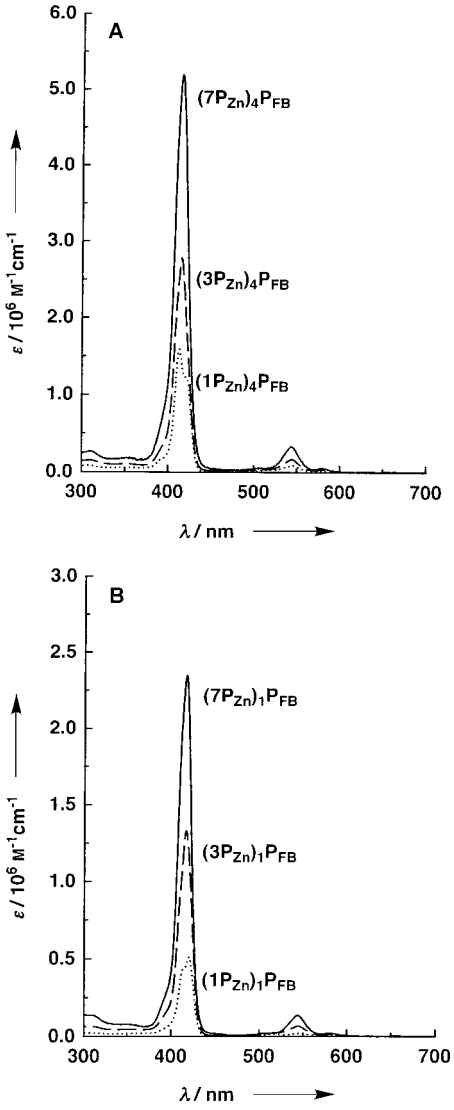

Figure 2. Electronic absorption spectra in THF at 25 °C of A) star-shaped $(1P_{Zn})_4P_{FB}$, $(3P_{Zn})_4P_{FB}$, and $(7P_{Zn})_4P_{FB}$, and B) cone-shaped $(1P_{Zn})_1P_{FB}$, $(3P_{Zn})_1P_{FB}$, and $(7P_{Zn})_1P_{FB}$.

Steady-state fluorescence spectroscopy: Upon excitation of the zinc porphyrin units (P_{Zn}) at $\lambda = 544$ nm in THF at 25 °C, the star-shaped multiporphyrin arrays all emitted a fluorescence from the free-base porphyrin (P_{FB}) focal core (658, 723 nm) with a negligibly weak emission from the P_{Zn} units (589, 623 nm) (Figure 3A, solid lines). In sharp contrast, their noncovalent references showed an emission from the P_{Zn} units almost exclusively (Figure 3A, broken lines). On the other hand, cone-shaped multiporphyrin arrays, such as $(3P_{Zn})_1P_{FB}$ and $(1P_{Zn})_1P_{FB}$ also emitted a fluorescence predominantly

  0947-6539/02/0812-2672 $ 20.00+.50/0 *Chem. Eur. J.* **2002**, *8*, No. 12

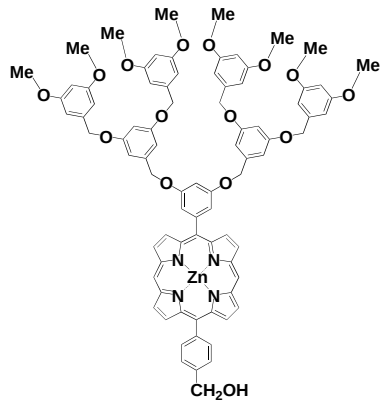

P_{Zn}^{EXT}

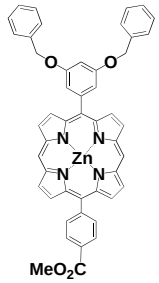

P_{Zn}^{INT}

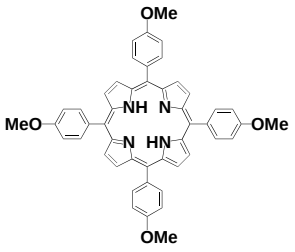

P_{FB}^{CORE}

from the P_{FB} unit (Figure 3B, solid lines). However, $(7P_{Zn})_1P_{FB}$, the largest homologue of this series, produced an emission mostly from the P_{Zn} units, whereas the emission from the P_{FB} focal core was rather weak.

$(1P_{Zn})_4$-ester-P_{FB} and $(3P_{Zn})_4$-ester-P_{FB} make use of ester linkages to connect (dendritic) zinc porphyrin (P_{Zn}) units to the free-base porphyrin (P_{FB}) focal core, and they are reference compounds for the ether-linked $(1P_{Zn})_4P_{FB}$ and $(3P_{Zn})_4P_{FB}$, respectively. Upon excitation at $\lambda =$ 544 nm, both multiporphyrin arrays emitted mostly from the P_{FB} core with a minor P_{Zn} fluorescence (Figure 3A, solid lines), although their noncovalent references ($P_{Zn}^{EXT}/P_{Zn}^{INT}/P_{FB}^{CORE} = 4:0:1$ and 8:4:1, respectively) again emitted mainly from the zinc porphyrin components P_{Zn}^{EXT} and P_{Zn}^{INT} with a negligibly weak fluorescence from P_{FB}^{CORE} (Figure 3A, broken lines). From the intensity ratios of the normalized P_{Zn} fluorescence of the covalent and noncovalent systems, the efficiencies of the P_{Zn}-to-P_{FB} energy transfer (Φ_{ENT}) were estimated[17] to be 86% for $(1P_{Zn})_4$-ester-P_{FB} ($(1P_{Zn})_4P_{FB}$, 87%) and 77% for $(3P_{Zn})_4$-ester-P_{FB} ($(3P_{Zn})_4P_{FB}$, 80%). Similarly to the ether-linked versions, cone-shaped $(3P_{Zn})_1$-ester-P_{FB} displayed much less efficient energy-transfer characteristics, where the comparison of its fluorescence intensity with that of the noncovalent reference ($P_{Zn}^{EXT}/P_{Zn}^{INT}/P_{FB}^{CORE} =$ 2:1:1) gave a Φ_{ENT} value of only 63% ($(3P_{Zn})_1P_{FB}$, 66%) (Figure 3B). From these results, it is likely that the ester and ether linkers are not much different from one another in energy transfer, although the former is conformationally less flexible than the latter.

Time-resolved fluorescence spectroscopy: In general, energy-transfer properties by a through-space (Förster) mechanism are dependent of the donor–acceptor (D–A) distance,[18] for which energy-transfer efficiency should decrease in inverse

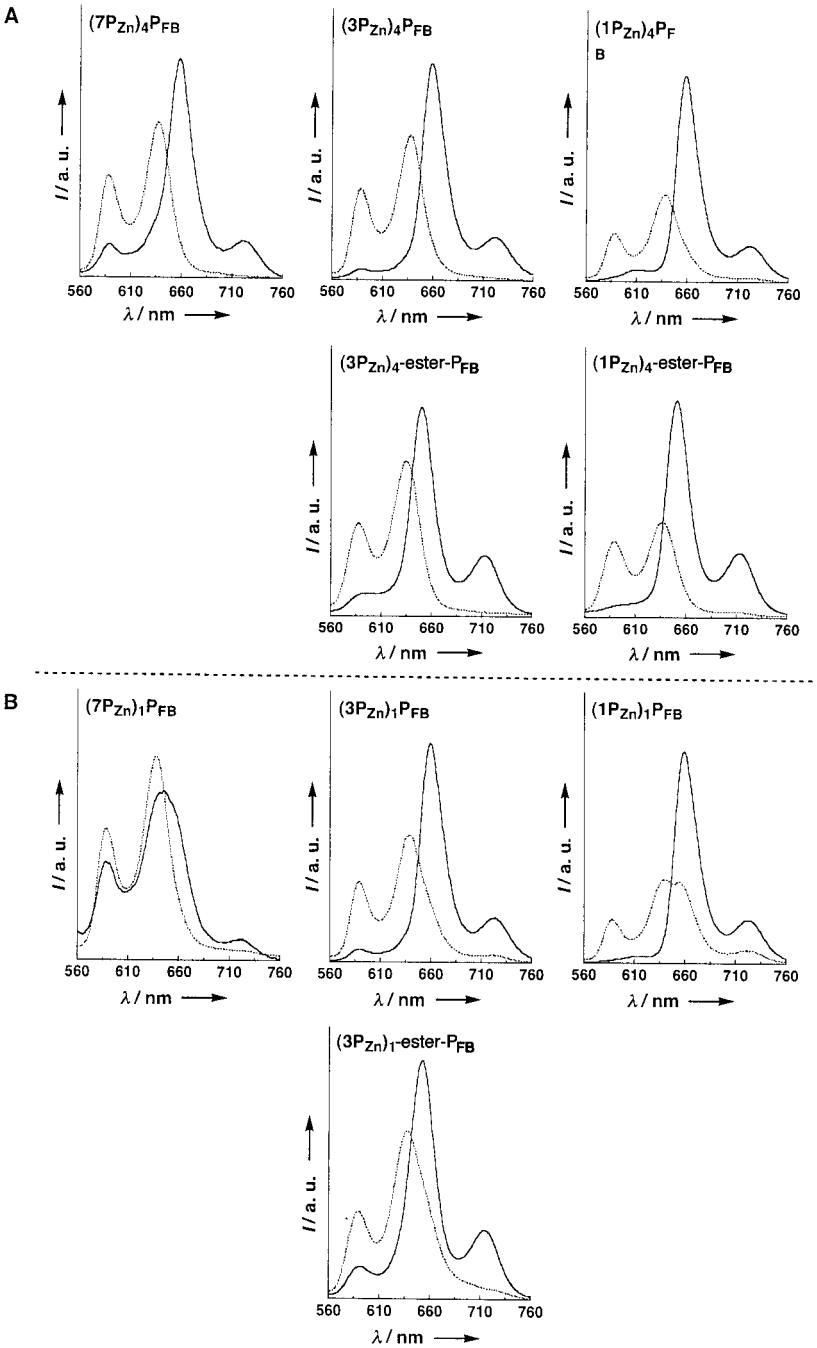

Figure 3. Steady-state fluorescence spectra in THF at 25°C of A) star-shaped $(1P_{Zn})_4P_{FB}$ [$(1P_{Zn})_4$-ester-P_{FB}], $(3P_{Zn})_4P_{FB}$ [$(3P_{Zn})_4$-ester-P_{FB}], and $(7P_{Zn})_4P_{FB}$, B) cone-shaped $(1P_{Zn})_1P_{FB}$, $(3P_{Zn})_1P_{FB}$ [$(3P_{Zn})_1$-ester-P_{FB}], and $(7P_{Zn})_1P_{FB}$, and their noncovalent references (broken lines) prepared by mixing P_{Zn}^{EXT}, P_{Zn}^{INT}, and P_{FB}^{CORE}. All spectra were normalized to a constant absorbance ($abs_{ext} = 0.02$) at the excitation wavelength ($\lambda_{ext} = 544$ nm).

proportion to the sixth power of the D–A distance. To investigate the dynamics of the intramolecular energy transfer events, fluorescence lifetimes of the P_{Zn} units in all the multiporphyrin arrays were measured in THF at 25 °C. Figure 4 shows time-resolved fluorescence decay profiles, monitored at $\lambda = 585$ nm, of the star-shaped and cone-shaped multiporphyrin arrays, upon excitation at $\lambda = 415$ nm. The fluorescence decay curves of porphyrin monomer $1P_{Zn}$ (R = CH_2OH) (= P_{Zn}^{EXT}) (Figure 4A, a reference for $(1P_{Zn})_4P_{FB}$ and

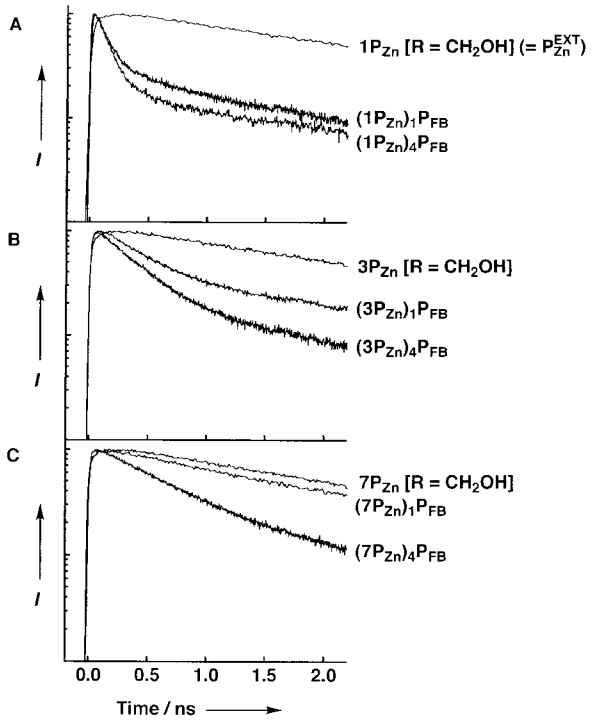

Figure 4. Fluorescence decay profiles monitored at $\lambda = 585$ nm of A) $1P_{Zn}$ [R = CH_2OH] (= P_{Zn}^{EXT}), $(1P_{Zn})_1P_{FB}$, and $(1P_{Zn})_4P_{FB}$, B) $3P_{Zn}$ [R = CH_2OH], $(3P_{Zn})_1P_{FB}$, and $(3P_{Zn})_4P_{FB}$, and C) $7P_{Zn}$ [R = CH_2OH], $(7P_{Zn})_1P_{FB}$, and $(7P_{Zn})_4P_{FB}$, upon excitation at $\lambda = 415$ nm in THF ($abs_{ext} < 0.1$) at 25 °C.

$(1P_{Zn})_1P_{FB}$), dendritic trimer $3P_{Zn}$ (R = CH_2OH) (Figure 4B, a reference for $(3P_{Zn})_4P_{FB}$ and $(3P_{Zn})_1P_{FB}$), and dendritic heptamer $7P_{Zn}$ (R = CH_2OH) (Figure 4C, a reference for $(7P_{Zn})_4P_{FB}$ and $(7P_{Zn})_1P_{FB}$), were also measured (formulae shown in Scheme 1). In these reference systems, which do not contain an energy-accepting free-base porphyrin (P_{FB}) focal core, the lifetimes of the zinc porphyrin fluorescence (τ_D) were evaluated to be ≈2.3 ns. In contrast, all the multiporphyrin arrays with a focal P_{FB} core showed a quenching signature of the zinc porphyrin fluorescence. As already reported,[13] the average lifetime of the photoexcited states of the P_{Zn} units (τ_{DA}^{av}) in star-shaped $(7P_{Zn})_4P_{FB}$ (680 ps) was much shorter than in cone-shaped $(7P_{Zn})_1P_{FB}$ (1899 ps), despite the fact that $(7P_{Zn})_4P_{FB}$ has a larger number of the P_{Zn} units located away from the energy-accepting focal P_{FB} core. For one generation lower, star-shaped $(3P_{Zn})_4P_{FB}$, the fluorescence decay profile was analyzed as a function of three exponential components, to give a τ_{DA}^{av} value of 456 ps, while cone-shaped $(3P_{Zn})_1P_{FB}$ gave a longer $\tau_{DA}^{av} = 801$ ps. On the other hand, the smallest homologues of the star- and cone-shaped series, $(1P_{Zn})_4P_{FB}$ and $(1P_{Zn})_4P_{FB}$, showed much shorter but almost identical τ_{DA}^{av} values, 329 and 308 ps, respectively. From these results, it is clear that the morphology of the chromophore array plays an important role in energy transfer when the generation number is high.

As shown in Figure 5, the star- and cone-shaped series displayed quite different dependencies of the photochemical properties on the generation number. In the case of the cone-shaped series, the population of a long-lived fluorescing

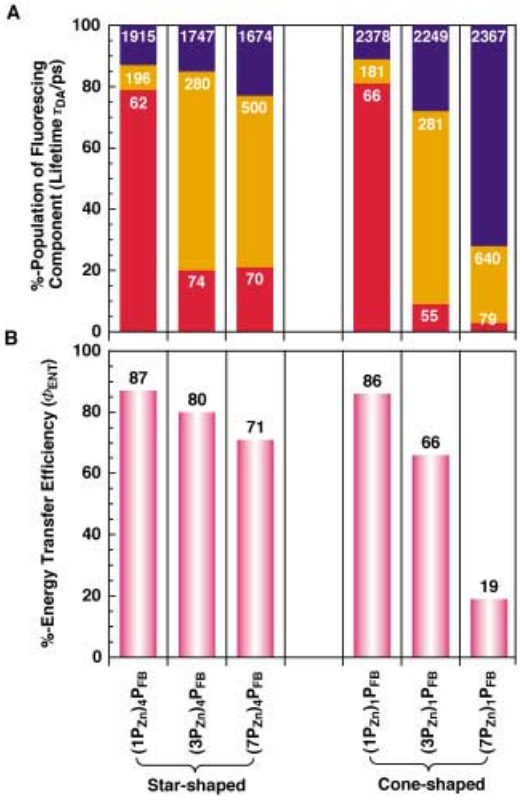

Figure 5. A) Populations [%] and lifetimes τ_{DA} [ps] of fluorescing components, and B) energy-transfer efficiencies [%], upon excitation at $\lambda = 415$ nm in THF ($abs_{ext} < 0.1$) at 25 °C. χ^2, τ_{DA} [ps]: 1.10, 308 for $(1P_{Zn})_4P_{FB}$; 1.07, 456 for $(3P_{Zn})_4P_{FB}$; 0.99, 680 for $(7P_{Zn})_4P_{FB}$ (star-shaped series), and 1.08, 329 for $(1P_{Zn})_1P_{FB}$; 1.05, 801 for $(3P_{Zn})_1P_{FB}$; 1.03, 1899 for $(7P_{Zn})_1P_{FB}$ (cone-shaped series). Rise-times of P_{FB} fluorescence: 49 ps for $(1P_{Zn})_4P_{FB}$; 70, 280 ps for $(3P_{Zn})_4P_{FB}$; 88, 345 ps for $(7P_{Zn})_4P_{FB}$, 138 ps for $(1P_{Zn})_1P_{FB}$; 204 ps for $(3P_{Zn})_1P_{FB}$; 80, 652 ps for $(7P_{Zn})_1P_{FB}$. The accuracies of τ_{DA} values were estimated to be ±5 ps.

component, assignable to a residual component in energy transfer, became considerably larger: it increased from 11 to 72% as the generation number of the dendritic wedge increased (Figure 5A). On the other hand, that of a short-lived fluorescing component with a τ_{DA} value of several tens of picoseconds decreased remarkably from 81 to 3%. Accordingly, the Φ_{ENT} value dropped off from 86% ($(1P_{Zn})_1P_{FB}$) to 66% ($(3P_{Zn})_1P_{FB}$), and then to 19% ($(7P_{Zn})_1P_{FB}$) (Figure 5B); the large gap in Φ_{ENT} between $(3P_{Zn})_1P_{FB}$ and the next generation $(7P_{Zn})_1P_{FB}$ suggests some limitation of σ-bonded chromophore arrays in long-range energy transfer. In sharp contrast, the star-shaped series bearing four dendritic zinc porphyrin wedges exhibited a much smaller dependency of the energy-transfer properties on the generation number,

0947-6539/02/0812-2674 $ 20.00+.50/0 Chem. Eur. J. 2002, 8, No. 12

whereby the Φ_{ENT} value of the highest generation $(7P_{Zn})_4P_{FB}$ remained at 71%,[13] which is much higher than that of cone-shaped $(7P_{Zn})_1P_{FB}$ with the same generation number, and even higher than that of one generation lower $(3P_{Zn})_1P_{FB}$. The fluorescence decay profile of $(7P_{Zn})_4P_{FB}$ still showed the presence of a considerable population (21%) of a short-lived ($\tau_{DA} = 70$ ps) fluorescing component, while that of the long-lived fluorescing component (23%) was not much different from that of the smallest $(1P_{Zn})_4P_{FB}$ (13%) (Figure 5A). Analysis of the transient fluorescence spectral change profiles, monitored at $\lambda = 723$ nm, gave rise-times of the free-base porphyrin (P_{FB}) fluorescence, the timescales of which, in most cases, agreed well with the observed lifetimes of the zinc porphyrin (P_{Zn}) fluorescing components in Figure 5A (see the caption). Thus, the decay of the P_{Zn} fluorescence is fundamentally a consequence of the energy transfer to the focal free-base porphyrin (P_{FB}) core. Although the rate constant of the P_{Zn}-to-P_{FB} energy transfer k_{ENT}, calculated according to the equation $k_{ENT} = (1/\tau_{DA}^{av}) - (1/\tau_D)$, was smaller in each series as the generation number was higher, a gap in k_{ENT} between star- and the corresponding cone-shaped analogues was considerably larger: 2.81×10^9 and $2.61 \times 10^9\ s^{-1}$ for the first-generation $(1P_{Zn})_4P_{FB}$ and $(1P_{Zn})_1P_{FB}$, 1.75×10^9 and $0.82 \times 10^9\ s^{-1}$ for the second-generation $(3P_{Zn})_4P_{FB}$ and $(3P_{Zn})_1P_{FB}$, and 1.04×10^9 and $0.10 \times 10^9\ s^{-1}$ for the third-generation $(7P_{Zn})_4P_{FB}$ and $(7P_{Zn})_1P_{FB}$ (Figure 6).

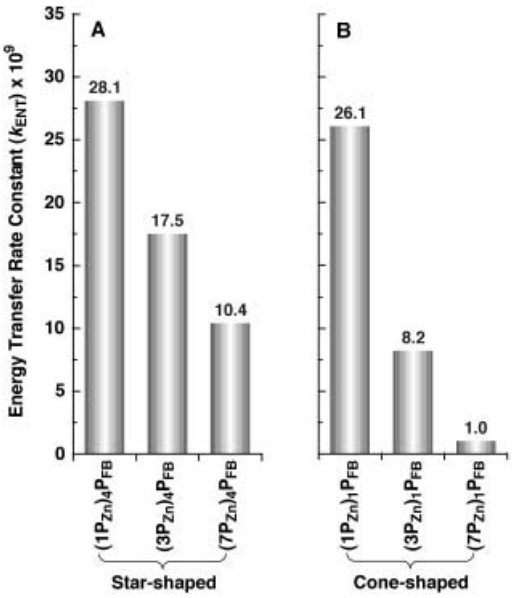

Figure 6. Energy-transfer rate constants (k_{ENT}) of A) star-shaped $(1P_{Zn})_4P_{FB}$, $(3P_{Zn})_4P_{FB}$, and $(7P_{Zn})_4P_{FB}$, and B) cone-shaped $(1P_{Zn})_1P_{FB}$, $(3P_{Zn})_1P_{FB}$, and $(7P_{Zn})_1P_{FB}$.

Light-harvesting activities of the multiporphyrin arrays should be evaluated both from the magnitude of the absorption cross section and the efficiency of vectorial energy transfer. Figure 7 shows relative light-harvesting activities of the multiporphyrin arrays, based on $(1P_{Zn})_1P_{FB}$, as evaluated from the molar extinction coefficients of the Soret absorption band ($\lambda = 415$ nm) (ε_{415}), multiplied by the P_{Zn}-to-P_{FB} energy-transfer efficiencies (Φ_{ENT}). For the star-shaped series, the

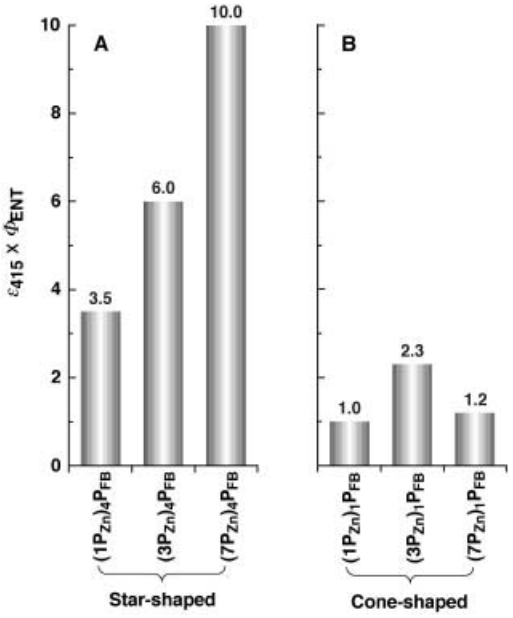

Figure 7. Light-harvesting activities of A) star-shaped $(1P_{Zn})_4P_{FB}$, $(3P_{Zn})_4P_{FB}$, and $(7P_{Zn})_4P_{FB}$, and B) cone-shaped $(1P_{Zn})_1P_{FB}$, $(3P_{Zn})_1P_{FB}$, and $(7P_{Zn})_1P_{FB}$, as evaluated from molar extinction coefficients at the excitation wavelength (ε_{415}), multiplied by energy-transfer efficiencies (Φ_{ENT}). All values $\varepsilon_{415} \times \Phi_{ENT}$ are normalized to that of $(1P_{Zn})_1P_{FB}$.

light-harvesting activity was considerably increased with the generation number of the dendritic wedges, for which a value $\varepsilon_{415}\Phi_{ENT}$ of $(7P_{Zn})_4P_{FB}$ was ten times as large as that of $(1P_{Zn})_1P_{FB}$. In sharp contrast, those of the cone-shaped series were all low and less dependent on the generation number. Therefore, star-shaped $(7P_{Zn})_4P_{FB}$ with 28 light-absorbing P_{Zn} units serves as an excellent energy funnel for visible light.

Fluorescence anisotropy: Analogous to the photochemical events in the bacterial light-harvesting antenna complexes, the P_{Zn}-to-P_{FB} energy transfer in the star-shaped series may be facilitated by a cooperative energy migration among the dendritic P_{Zn} units, thereby the photochemical events can compete with a radiative decay to the ground state. Figure 8 shows steady-state fluorescence depolarization characteristics of some selected multiporphyrin arrays, upon excitation with a polarized light at $\lambda = 544$ nm ($abs_{ext} = 0.03$) at 25 °C, in polyethylene glycol ($MW = 200$) containing THF. In such a viscous medium, molecular rotation is suppressed, and the fluorescence depolarization is likely to occur mostly by means of energy migration among randomly oriented chromophore units in the dendritic array. Under the above conditions, a monomeric zinc porphyrin, such as P_{Zn}^{EXT}, showed a degree of fluorescence polarization $P = (I_{\parallel} - GI_{\perp})/(I_{\parallel} + GI_{\perp})$ of 0.19, in which $I_{\parallel}$ and $I_{\perp}$ are fluorescence intensities observed through polarizers oriented parallel and perpendicular, respectively, to a vertically polarized excitation light. As already reported,[13] star-shaped $(7P_{Zn})_4P_{FB}$ emits a highly depolarized fluorescence from the P_{Zn} units, for which the P value is only as low as 0.03. In contrast, cone-shaped $(7P_{Zn})_1P_{FB}$ has a much higher P value (0.10) than $(7P_{Zn})_4P_{FB}$, indicating a less efficient energy migration over the dendritic P_{Zn} units. The same was true for the fluorescence depolarization characteristics of one gener-

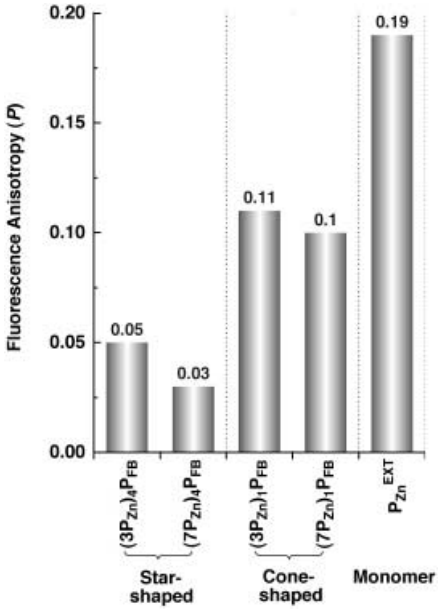

Figure 8. Anisotropies of the zinc porphyrin fluorescence (P) at $\lambda =$ 585 nm of star-shaped $(3P_{Zn})_4P_{FB}$ and $(7P_{Zn})_4P_{FB}$, cone-shaped $(3P_{Zn})_1P_{FB}$ and $(7P_{Zn})_1P_{FB}$, and monomeric zinc porphyrin P_{Zn}^{EXT} as reference, upon excitation at $\lambda = 544$ nm ($abs_{ext} = 0.03$) at 25 °C with a polarized light under Ar in polyethylene glycol ($MW = 200$) containing THF.

ation lower $(3P_{Zn})_4P_{FB}$ ($P = 0.05$) and $(3P_{Zn})_1P_{FB}$ ($P = 0.11$), although the observed fluorescence anisotropies were both higher than that of $(7P_{Zn})_4P_{FB}$. These trends indicate a morphology-assisted cooperative energy migration among the zinc porphyrin (P_{Zn}) units, which must be responsible for the high efficiency of the long-range P_{Zn}-to-P_{FB} energy transfer in the star-shaped dendritic multiporphyrin arrays.

Conclusion

In the present paper, we demonstrate that a dendritic architecture is a highly promising candidate as a scaffold for molecular design of light-harvesting antennae that can incorporate a large number of chromophore units and also allows them to cooperate in energy migration, leading to a highly efficient energy transfer to the focal chromophore unit. In particular, star-shaped dendritic chromophore arrays, in which the chromophore units could be arranged in an analogous fashion to those in the natural light-harvesting antenna complexes, can cope with both a large absorption cross section and a high efficiency of vectorial energy transfer. Such a molecular design approach possibly provides a new strategy toward artificial photosynthesis, which is a subject of great importance for science and technology in this century. As can be seen from this study, the combination of large, dendritic light-harvesting antenna units with electron-transfer relay systems is one of the subjects worthy of further investigation.

Experimental Section

Materials: Dichloromethane (CH_2Cl_2) was washed successively with concentrated H_2SO_4, water, and aqueous $NaHCO_3$, dried over $CaCl_2$, and then distilled over CaH_2 under Ar just before use. Tetrahydrofuran (THF), used as a solvent for synthetic reactions, was distilled from sodium benzophenone under Ar just before use. Chloroform ($CHCl_3$) and methanol (MeOH), for the synthesis of monomeric porphyrins, were used as-received from Shin Etsu. [18]Crown-6 ether was recrystallized from acetonitrile (MeCN). Potassium carbonate (K_2CO_3) and potassium fluoride (KF) were kept in an oven at 130 °C. Commercially available reagents, such as 5,10,15,20-tetrakis(4-hydroxyphenyl)porphine ($(HO)_4P_{FB}$) and 5,10,15,20-tetrakis(4-carboxyphenyl)porphine ($(HO_2C)_4P_{FB}$) were used as-received from TCI and Aldrich, respectively.

Syntheses: Monomeric porphyrins, such as $(HO)_1(MeO)_3P_{FB}$ and $(HO)_2P_{Zn}(CO_2Me)$, dendritic zinc porphyrins, such as $1P_{Zn}$ ($R = CH_2Br$), $3P_{Zn}$ ($R = CH_2Br$), and $7P_{Zn}$ ($R = CH_2Br$), and cone and star-shaped, large multiporphyrin arrays, such as $(7P_{Zn})_1P_{FB}$ and $(7P_{Zn})_4P_{FB}$, were synthesized according to the methods reported previously (Scheme 1).[13]

Measurements: Recycling preparative HPLC was carried out on a Japan Analytical Industry model LC-908, equipped with a column set consisting of JAIGEL-2H (exclusion limit 5×10^3) combined with JAIGEL-1H (exclusion limit 1×10^3) or JAIGEL-3H (exclusion limit 3×10^4), with $CHCl_3$ as the eluent at a flow rate of 3.5 mL min^{-1}. MALDI-TOF MS was performed on a PerSeptive Biosystems model Voyager-DE spectrometer with dithranol as the matrix. ^{1}H NMR spectroscopy was performed in $CDCl_3$ or CD_3OD on a JEOL GSX-270 spectrometer operating at 270 MHz. The chemical shifts were determined with respect to $CHCl_3$ ($\delta = 7.28$) or MeOH ($\delta = 4.7$) as the internal standard. Electronic absorption spectra were recorded at 25 °C on a JASCO model V-570 spectrophotometer in a quartz cell of 1 cm path length. Fluorescence spectra were recorded at 25 °C in a quartz cell of 1 cm path length, on a JASCO model FP-777W spectrophotometer equipped with a temperature controller, and corrected for wavelength-dependent detector sensitivity and excitation light source output. Time-resolved fluorescence spectra and fluorescence decay profiles were measured at 25 °C with a picosecond pulse laser and a single-photon timing apparatus. The laser system was a Coherent model Mira 900 mode-locked Ti-sapphire laser, pumped by a Coherent model Innova 300 Ar-ion laser combined with a Coherent model 9200 pulse picker. Decay curves were obtained with an excitation wavelength of 415 nm by means of a Hamamatsu model R2809U-01 microchannel-plate photomultiplier. The pulse width of instrumental response function was 30 ps (FWHM). The accuracies of lifetime values thus evaluated were estimated to be ±2 ps for single exponential decays and ±5 ps in multiexponential decays. Degree of fluorescence polarization (P) was calculated according to the equation $P = (I_{\parallel} - GI_{\perp})/(I_{\parallel} + GI_{\perp})$, in which $I_{\parallel}$ and $I_{\perp}$ are fluorescence intensities observed through polarizers oriented parallel and perpendicular to a vertically polarized excitation light, respectively, and G, given by $i_{\parallel}/i_{\perp}$, is an instrumental correction factor for depolarization effects arising from the instrument, for which $i_{\parallel}$ and $i_{\perp}$ denote fluorescence intensities observed through polarizers.

$(1P_{Zn})_1P_{FB}$: A solution of $(HO)_1(MeO)_3P_{FB}$ (6.4 mg, 8.8 μmol), $1P_{Zn}$ ($R = CH_2Br$; 16.4 mg, 10.9 μmol), and anhydrous K_2CO_3 (2.5 mg, 18.1 μmol) in *N*-methylpyrrolidone (1 mL) was heated at 80 °C under Ar for 12 h in the dark. The reaction mixture was poured into water (10 mL) and extracted with $CHCl_3$ (3 × 20 mL). The combined extract was washed with water (3 × 50 mL), dried over Na_2SO_4, and evaporated to dryness. The residue was subjected to recycling preparative SEC with $CHCl_3$ as the eluent. The first fraction was collected and evaporated to dryness to give $(1P_{Zn})_1P_{FB}$ as a red solid in 53% yield (10 mg). ^{1}H NMR (270 MHz, $CDCl_3$, 25 °C): $\delta = -2.67$ (s, 2H; NH), 3.70 (s, 24H; dendron-Ar$(OCH_3)_2$), 4.13 (s, 9H; P_{FB}-ArOCH_3), 4.98 (s, 8H; outer dendron-CH_2O), 5.23 (s, 4H; inner dendron-CH_2O), 5.77 (s, 2H; CH_2O between P_{Zn} units), 6.33 (s, 8H; *p*-H in outer dendron-C_6H_3), 6.53 (s, 16H; *o*-H in outer dendron-C_6H_3), 6.64 (s, 4H; *p*-H in inner dendron-C_6H_3), 6.79 (s, 8H; *o*-H in inner dendron-C_6H_3), 7.01 (s, 1H; *p*-H in P_{Zn}-C_6H_3), 7.33 (d, $J = 6.4$ Hz, 6H; *m*-H in P_{FB}-C_6H_4), 7.56 (s, 2H; *o*-H in P_{Zn}-C_6H_3), 7.62 (d, $J = 8.5$ Hz, 2H; *m*-H in P_{FB}-C_6H_4), 8.09 (d, $J = 7.9$ Hz, 2H; *o*-H in P_{FB}-C_6H_4), 8.18 (d, $J = 8.3$ Hz, 6H; *o*-H in P_{FB}-C_6H_4), 8.30 (d, $J = 7.9$ Hz, 2H; *m*-H in P_{Zn}-C_6H_4), 8.43 (d, $J = 8$ Hz, 2H; *o*-H in P_{Zn}-C_6H_4), 8.91–9.00 (m, 8H; pyrrole-*β*-H in P_{FB}), 9.18 (d, $J = 4.5$ Hz, 2H; pyrrole-*β*-H in P_{Zn}), 9.27 (d, $J = 4.5$ Hz, 2H; pyrrole-*β*-H in P_{Zn}), 9.43 (d, $J = 4.7$ Hz, 2H; pyrrole-*β*-H in P_{Zn}), 9.50 (d, $J = 4.5$ Hz, 2H; pyrrole-*β*-H in P_{Zn}), 10.34 ppm (s, 2H; *meso*-H in P_{Zn}); MALDI-TOF MS: calcd for $C_{130}H_{109}N_8O_{18}Zn$ [M^++H]: 2135; found: 2135; UV/Vis (THF, 25 °C): λ_{max} (ε) = 420.2 (495 000), 517.3, 545.9 nm (7000 M^{-1} cm^{-1}).

  0947-6539/02/0812-2676 $ 20.00+.50/0 *Chem. Eur. J.* **2002**, *8*, No. 12

$(1P_{Zn})_4P_{FB}$: A solution of $(HO)_4P_{FB}$ (4.0 mg, 5.9 μmol), $1P_{Zn}$ (R = CH_2Br, 43.3 mg, 29.0 μmol), and anhydrous K_2CO_3 (8.1 mg, 59.0 μmol) in *N*-methylpyrrolidone (1 mL) was heated at 80 °C under Ar for 24 h in the dark. The reaction mixture was treated in a manner similar to that for $(1P_{Zn})_1P_{FB}$ to give $(1P_{Zn})_4P_{FB}$ as a red solid in 62% yield (23 mg). ^{1}H NMR (270 MHz, $CDCl_3$, 25 °C): $\delta = -2.47$ (s, 2H; NH), 3.61 (s, 96H; dendron-Ar(OCH_3)$_2$), 4.81 (s, 32H; outer dendron-CH_2O), 5.09 (s, 16H; inner dendron-CH_2O), 5.53 (s, 8H; CH_2O between P_{Zn} and P_{FB}), 6.22 (s, 16H; *p*-H in outer dendron-C_6H_3), 6.38 (d, $J = 1.7$ Hz, 32H; *o*-H in outer dendron-C_6H_3), 6.50 (s, 8H; *p*-H in inner dendron-C_6H_3), 6.66 (s, 16H; *o*-H in inner dendron-C_6H_3), 7.00 (s, 4H; *p*-H in P_{Zn}-C_6H_3), 7.51 (s, 16H; *o*-H and *m*-H in P_{FB}-C_6H_4), 7.88 (s, 8H; *o*-H in P_{Zn}-C_6H_3), 8.31 (s, 16H; *o*-H and *m*-H in P_{Zn}-C_6H_4), 9.09 (s, 8H; pyrrole-β-H in P_{FB}), 9.17 (t, $J = 4$ Hz, 16H; pyrrole-β-H in P_{Zn}), 9.37 (t, $J = 4.9$ Hz, 16H; pyrrole-β-H in P_{Zn}), 10.24 ppm (s, 8H; *meso*-H in P_{Zn}); MALDI-TOF MS: calcd for $C_{376}H_{318}N_{20}O_{60}Zn_4$ [M^++H]: 6337; found: 6337; UV/Vis (THF, 25 °C): λ_{max} (ε) = 413.0 (1584000), 545.2 nm (39000 $M^{-1}cm^{-1}$).

$(3P_{Zn})_1P_{FB}$: A solution of $(HO)_1(MeO)_3P_{FB}$ (3.0 mg, 4.2 μmol), $3P_{Zn}$ (R = CH_2Br, 17.4 mg, 5.0 μmol), and anhydrous K_2CO_3 (1.2 mg, 8.4 μmol) in *N*-methylpyrrolidone (0.5 mL) was heated at 80 °C under Ar for 12 h in the dark. The reaction mixture was treated in a manner similar to that for $(1P_{zn})_1P_{FB}$ to give $(3P_{Zn})_1P_{FB}$ as a red solid in 31% yield (5.4 mg). ^{1}H NMR (270 MHz, $CDCl_3$, 25 °C): $\delta = -2.77$ (s, 2H; NH), 3.62 (s, 48H; dendron-Ar(OCH_3)$_2$), 4.09 (d, $J = 9$ Hz, 9H; P_{FB}-Ar OCH_3), 4.87 (s, 16H; outer dendron-CH_2O), 5.16 (s, 8H; inner dendron-CH_2O), 5.72 (s, 4H; CH_2O between P_{Zn} units), 5.91 (s, 2H; CH_2O between P_{Zn} and P_{FB}), 6.23 (t, $J =$ 2.1 Hz, 8H; *p*-H in outer dendron-C_6H_3), 6.43 (d, $J = 2.5$ Hz, 16H; *o*-H in outer dendron-C_6H_3), 6.56 (t, $J = 2.1$ Hz, 4H; *p*-H in inner dendron-C_6H_3), 6.73 (d, $J = 2.1$ Hz, 8H; *o*-H in inner dendron-C_6H_3), 7.05 (s, 2H; *p*-H in outer P_{Zn}-C_6H_3), 7.50 (s, 1H; *p*-H in inner P_{Zn}-C_6H_3), 7.52 (d, $J = 2.1$ Hz, 4H; *o*-H in outer P_{Zn}-C_6H_3), 7.89 (d, $J = 2.1$ Hz, 2H; *o*-H in inner P_{Zn}-C_6H_3), 8.33 (m, 12H; *m*-, *p*-H in P_{Zn}-C_6H_4), 8.42 (m, 16H; *m*-, *p*-H in P_{FB}-C_6H_4), 8.84–8.93 (m, 8H; pyrrole-β-H in P_{FB}), 9.11–9.27 (m, 24H; pyrrole-β-H in P_{Zn}), 10.07 (s, 4H; *meso*-H in outer P_{Zn}), 10.33 ppm (s, 2H; *meso*-H in inner P_{Zn}); MALDI-TOF MS: calcd for $C_{246}H_{200}N_{16}O_{34}Zn_3$ [M^++H]: 4119; found: 4120; UV/Vis (THF, 25 °C): λ_{max} (ε) = 416.5 (1319000), 545.2 nm (30000 $M^{-1}cm^{-1}$).

$(3P_{Zn})_4P_{FB}$: A solution of $(HO)_4P_{FB}$ (2.0 mg, 3.0 μmol), $3P_{Zn}$ (R = CH_2Br, 51.1 mg, 14.7 μmol), and anhydrous K_2CO_3 (4.2 mg, 30.0 μmol) in *N*-methylpyrrolidone (1 mL) was heated at 80 °C under Ar for 72 h in the dark. The reaction mixture was treated in a manner similar to that for $(1P_{Zn})_1P_{FB}$ to give $(3P_{Zn})_4P_{FB}$ as a red solid in 20% yield (15 mg). The ^{1}H NMR spectrum was rather broad, even at an elevated temperature of 55 °C, possibly caused by a much slower conformational change than the NMR timescale. ^{1}H NMR (270 MHz, $CDCl_3$, 55 °C): $\delta = -2.84$ (s, 2H; NH), 3.31 (s, 192H; dendron-Ar(OCH_3)$_2$), 4.50 (s, 64H; outer dendron-CH_2O), 4.88 (s, 32H; inner dendron-CH_2O), 5.14 (s, 16H; CH_2O between P_{Zn} units), 5.88 (s, 40H; *p*-H in outer dendron-C_6H_3, CH_2O between P_{Zn} and P_{FB}), 6.06 (s, 64H; *o*-H in outer dendron-C_6H_3), 6.24 (s, 16H; *p*-H in inner dendron-C_6H_3), 6.44 (s, 8H; *o*-H in inner dendron-C_6H_3), 6.85 (s, 12H; *p*-H in P_{Zn}-C_6H_3), 7.38 (s, 24H; *o*-H in P_{Zn}-C_6H_3), 7.48 and 7.87 (s, 48H; P_{Zn}-C_6H_4), 8.72 and 8.95 (s, 104H; pyrrole-β-H in P_{Zn} and P_{FB}), 9.53 ppm (s, 24H; *meso*-H in P_{Zn}); MALDI-TOF MS: calcd for $C_{840}H_{686}N_{52}O_{124}Zn_{12}$ [M^++H]: 14274; found: 14276; UV/Vis (THF, 25 °C): λ_{max} (ε) = 415.7 (2723000), 545.3 nm (61000 $M^{-1}cm^{-1}$).

$(t$BuPh$_2$Si$)_2P_{Zn}$ (R = CO_2Me): *tert*-Butyldiphenylchlorosilane (tBuPh$_2$SiCl; 0.5 mL, 1.95 mmol) was slowly added to a solution of $(HO)_2P_{Zn}(CO_2Me)$ (0.40 g, 0.65 mmol) and imidazole (0.11 g, 1.62 mmol) in dry DMF (1 mL) while stirring vigorously at 4 °C for 1 h under N_2, and the mixture was stirred for 12 h at room temperature. The reaction mixture was then poured into aqueous $NaHCO_3$ (50 mL) and extracted with $CHCl_3$ (3 × 50 mL). The combined extracts were washed with water (3 × 50 mL), dried over Na_2SO_4, and evaporated to dryness. The residue was subjected to column chromatography on silica gel with CH_2Cl_2 as the eluent. The first fraction was collected and evaporated to dryness. The residue was freeze-dried from benzene to give (tBuPh$_2$Si)$_2P_{Zn}$ (R = CO_2Me) as a bright red powder in 52% yield (0.37 g). ^{1}H NMR (270 MHz, $CDCl_3$, 25 °C): $\delta = 1.13$ (s, 18H; $(CH_3)_3CSi$), 4.15 (s, 3H; CO_2CH_3), 6.84 (t, $J = 2.1$ Hz, 1H; *p*-H in P_{Zn}-C_6H_3), 7.22 (d, $J = 2.1$ Hz, 2H; *o*-H in P_{Zn}-C_6H_3), 7.36–7.47, 7.71–7.77 (m, 20H; $(C_6H_5)_2Si$), 8.33 (d, $J = 8.5$ Hz, 2H; *m*-H in P_{Zn}-C_6H_4), 8.47 (d, $J =$ 8.5 Hz, 2H; *o*-H in P_{Zn}-C_6H_4), 8.67 (d, $J = 4.3$ Hz, 2H; pyrrole-β-H in P_{Zn}), 9.04 (d, $J = 4.7$ Hz, 2H; pyrrole-β-H in P_{Zn}), 9.28 (d, $J = 4.7$ Hz, 2H; pyrrole-β-H in P_{Zn}), 9.42 (d, $J = 4.7$ Hz, 2H; pyrrole-β-H in P_{Zn}), 10.26 ppm (s, 2H; *meso*-H in P_{Zn}); MALDI-TOF MS: calcd for $C_{66}H_{59}N_4O_4Si_2Zn$ [M^++H]: 1093; found: 1093.

(tBuPh$_2$Si$)_2P_{Zn}$ (R = CH$_2$OH): $LiAlH_4$ (25 mg, 0.66 mmol) as a suspension in THF (2 mL) was added over a period of 0.5 h to a solution of (tBuPh$_2$Si$)_2P_{Zn}$ (R = CO_2Me; 0.36 g, 0.33 mmol) in dry THF (5 mL), while stirring vigorously, at 4 °C under N_2, and the mixture was stirred for 1 h at room temperature. The reaction mixture was then poured into ice-water (50 mL) and extracted with $CHCl_3$ (3 × 20 mL). The combined extracts were washed with water (3 × 50 mL), dried over Na_2SO_4, and evaporated to dryness. The residue was subjected to column chromatography on silica gel with CH_2Cl_2 as the eluent. The second fraction was collected and evaporated to dryness. The residue was freeze-dried from benzene containing a few drops of MeOH to give (tBuPh$_2$Si$)_2P_{Zn}$ (R = CH_2OH) as a bright red powder in 73% yield (0.27 g). ^{1}H NMR (270 MHz, $CDCl_3$, 25 °C): $\delta = 1.12$ (s, 18H; $(CH_3)_3CSi$), 5.04 (s, 2H; CH_2OH), 6.83 (s, 1H; *p*-H in P_{Zn}-C_6H_3), 7.22 (s, 2H; *o*-H in P_{Zn}-C_6H_3), 7.38–7.76 (m, 22H; $(C_6H_5)_2Si$, *m*-H in P_{Zn}-C_6H_4), 8.25 (d, $J = 7.7$ Hz, 2H; *o*-H in P_{Zn}-C_6H_4), 8.67 (d, $J =$ 4.3 Hz, 2H; pyrrole-β-H in P_{Zn}), 9.11 (d, $J = 4.3$ Hz, 2H; pyrrole-β-H in P_{Zn}), 9.28 (d, $J = 4.3$ Hz, 2H; pyrrole-β-H in P_{Zn}), 9.41 (d, $J = 4.3$ Hz, 2H; pyrrole-β-H in P_{Zn}), 10.23 ppm (s, 2H; *meso*-H in P_{Zn}); MALDI-TOF-MS: calcd for $C_{65}H_{59}N_4O_3Si_2Zn$ [M^++H]: 1065; found: 1064).

[(tBuPh$_2$Si)$_2P_{Zn}]_4$-ester-P_{FB}: Oxalyl chloride (10.3 μL, 0.12 mmol) was slowly added to a suspension of $(HO_2C)_4P_{FB}$ (9.5 mg, 12 μmol) in CH_2Cl_2 (1 mL) under N_2, while stirring vigorously, at 4 °C. After 1 h, MALDI-TOF MS of the reaction mixture showed a molecular ion peak corresponding to $[ClC(O)]_4P_{FB}$ (calcd for $C_{48}H_{27}Cl_4N_4O_4$ [M+H]$^+$: 865; found: 864). The reaction mixture was evaporated to dryness, and the residue was further dried with a vacuum pump for 3 h to remove excess oxalyl chloride. Then, (tBuPh$_2$Si$)_2P_{Zn}$ (R = CH_2OH) (51.8 mg, 60 μmol) and 4-dimethylaminopyridine (14.7 mg, 0.12 mmol) were added to the residue. The mixture was dissolved in dry CH_2Cl_2 (1 mL) at 4 °C, stirred for 12 h at room temperature, poured into aqueous $NaHCO_3$ (50 mL), and extracted with $CHCl_3$ (3 × 50 mL). The combined extracts were washed with water (3 × 50 mL), dried over Na_2SO_4, and evaporated to dryness. The residue was subjected to flash column chromatography on silica gel with CH_2Cl_2 as the eluent. The first fraction was collected and evaporated to dryness. The residue was then subjected to recycling preparative SEC with $CHCl_3$ as the eluent. The first fraction was collected and evaporated to dryness, and freeze-dried from benzene to give [(tBuPh$_2$Si$)_2P_{Zn}]_4$-ester-P_{FB} as a bright red powder in 57% yield (34 mg). ^{1}H NMR (270 MHz, $CDCl_3$, 25 °C): $\delta = -2.65$ (s, 2H; NH), 1.12 (s, 72H; $(CH_3)_3CSi$), 5.96 (s, 8H; CH_2O between P_{Zn} and P_{FB}), 6.83 (t, $J = 2.1$ Hz, 4H; *p*-H in P_{Zn}-C_6H_3), 7.21 (d, $J = 2.1$ Hz, 8H; *o*-H in P_{Zn}-C_6H_3), 7.34–7.48, 7.73–7.76 (m, 80H; $(C_6H_5)_2Si$), 8.02 (d, $J = 8.1$ Hz, 8H; *m*-H in P_{Zn}-C_6H_4), 8.34 (d, $J = 8.1$ Hz, 8H; *o*-H in P_{Zn}-C_6H_4), 8.48 (d, $J = 8.1$ Hz, 8H; *m*-H in P_{FB}-C_6H_4), 8.63 (d, $J = 4.7$ Hz, 8H; pyrrole-β-H in P_{Zn}), 8.72 (d, $J = 8.5$ Hz, 8H; *o*-H in P_{FB}-C_6H_4), 8.99 (s, 8H; pyrrole-β-H in P_{FB}), 9.13 (d, $J = 4.7$ Hz, 8H; pyrrole-β-H in P_{Zn}), 9.21 (d, $J = 4.7$ Hz, 8H; pyrrole-β-H in P_{Zn}), 9.37 (d, $J = 4.3$ Hz, 8H; pyrrole-β-H in P_{Zn}), 10.17 ppm (s, 8H; *meso*-H in P_{Zn}); MALDI-TOF MS: calcd for $C_{308}H_{255}N_{20}O_{16}Si_8Zn_4$ [M^++H]: 4977; found: 4981.

$(1P_{Zn})_4$-ester-P_{FB}: A solution of [(tBuPh$_2$Si$)_2P_{Zn}]_4$-ester-P_{FB} (20.0 mg, 4.0 μmol), poly(benzyl ether) dendritic bromide (L2-Br; 25 mg, 50 μmol), and anhydrous KF (9.3 mg, 0.16 mmol) in *N*-methylpyrrolidone (1 mL) was heated at 80 °C under Ar for 1 week in the dark. The reaction mixture was treated in a manner similar to that for the preparation of $(1P_{Zn})_4P_{FB}$ to give $(1P_{Zn})_4$-ester-P_{FB} as a red powder in 60% yield (15 mg). ^{1}H NMR (270 MHz, $CDCl_3$, 25 °C): $\delta = -2.69$ (s, 2H; NH), 3.60 (s, 96H; dendron-Ar(OCH_3)$_2$), 4.84 (s, 32H; outer dendron-CH_2O), 5.15 (s, 16H; inner dendron-CH_2O), 5.94 (s, 8H; CH_2O between P_{Zn} and P_{FB}), 6.20 (t, $J =$ 2.1 Hz, 16H; *p*-H in outer dendron-C_6H_3), 6.39 (d, $J = 2.1$ Hz, 32H; *o*-H in outer dendron-C_6H_3), 6.54 (s, 8H; *p*-H in inner dendron-C_6H_3), 6.71 (s, 16H; *o*-H in inner dendron-C_6H_3), 7.06 (s, 4H; *p*-H in P_{Zn}-C_6H_3), 7.50 (s, 16H; *o*-H and *m*-H in P_{FB}-C_6H_4), 8.02 (d, $J = 8.1$ Hz, 8H; *o*-H in P_{Zn}-C_6H_3), 8.37 (s, 16H; *o*-H and *m*-H in P_{Zn}-C_6H_4), 8.69 (d, $J = 4.7$ Hz, 8H; pyrrole-β-H in P_{FB}), 9.10 (d, $J = 4.7$ Hz, 8H; pyrrole-β-H in P_{Zn}), 9.18 (d, $J = 4.7$ Hz, 8H; pyrrole-β-H in P_{Zn}), 9.27 (d, $J = 4.7$ Hz, 8H; pyrrole-β-H in P_{Zn}), 9.40 (d, $J = 4.3$ Hz, 8H; pyrrole-β-H in P_{Zn}), 10.17 ppm (s, 8H; *meso*-H in P_{Zn}); MALDI-TOF MS: calcd for $C_{380}H_{319}N_{20}O_{64}Zn_4$ [M^++H]: 6449; found:

6452; UV/Vis (THF, 25 °C): λ_{max} (ε) = 413.5 (1 340 000 M^{-1}cm^{-1}), 514.5, 544.5, 581.5 nm.

$(3P_{Zn})_1$-ester-P_{FB}: Oxalyl chloride (16 μL, 0.19 mmol) was added slowly to a suspension of $(HO_2C)_4P_{FB}$ (15 mg, 19 μmol) in CH_2Cl_2 (3 mL) under N_2, while stirring vigorously, at 4 °C. After 1 h, MALDI-TOF MS of the reaction mixture showed a molecular ion peak corresponding to $[ClC(O)]_4P_{FB}$ (864 $[M+H]^+$; calcd for $C_{48}H_{27}Cl_4N_4O_4$: 865). The reaction mixture was evaporated to dryness, and the residue was further dried with a vacuum pump for 3 h to remove excess oxalyl chloride. Then, $3P_{Zn}$ (R = CH_2OH; 85 mg, 25 μmol) and 4-dimethylaminopyridine (23 mg, 0.19 mmol) were added to the residue, and the mixture was dissolved in dry CH_2Cl_2 (2 mL) at 4 °C. After stirring for 12 h at room temperature, MeOH (1 mL) was added to the reaction mixture to convert residual acid chloride into the methyl ester. The reaction mixture was treated in a manner similar to that for the preparation of $[(t\mathrm{BuPh_2Si})_2P_{Zn}]_4$-ester-$P_{FB}$ to give $(3P_{Zn})_1$-ester-P_{FB} as a bright red powder in 50 % yield (40 mg). ^{1}H NMR (270 MHz, $CDCl_3$, 25 °C): $\delta = -2.78$ (s, 2H; NH), 3.58 (s, 48H; dendron-Ar$(OCH_3)_2$), 4.01 (s, 9H; P_{FB}-ArOCH_3), 4.83 (s, 16H; outer dendron-CH_2O), 5.14 (s, 8H; inner dendron-CH_2O), 5.68 (s, 4H; CH_2O between P_{Zn} units), 5.77 (s, 2H; CH_2O between P_{Zn} and P_{FB}), 6.19 (t, J = 2.1 Hz, 8H; *p*-H in outer dendron-C_6H_3), 6.38 (d, J = 2.1 Hz, 16H; *o*-H in outer dendron-C_6H_3), 6.51 (t, J = 2.1 Hz, 4H; *p*-H in inner dendron-C_6H_3), 6.69 (d, J = 2.1 Hz, 8H; *o*-H in inner dendron-C_6H_3), 7.04 (t, J = 2.1 Hz, 2H; *p*-H in outer P_{Zn}-C_6H_3), 7.45 (s, 1H; *p*-H in inner P_{Zn}-C_6H_3), 7.51 (d, J = 2.1 Hz, 4H; *o*-H in outer P_{Zn}-C_6H_3), 7.84 (d, J = 1.7 Hz, 2H; *o*-H in inner P_{Zn}-C_6H_3), 8.26 – 8.54 (m, 32H; P_{FB}-C_6H_4, P_{Zn}-C_6H_4), 8.91 – 8.99 (m, 8H; pyrrole-*β*-H in P_{FB}), 9.06 – 9.27 (m, 24H; pyrrole-*β*-H in P_{Zn}), 9.98 (s, 4H; *meso*-H in outer P_{Zn}), 10.17 ppm (s, 2H; *meso*-H in inner P_{Zn}); MALDI-TOF MS: calcd for $C_{250}H_{201}N_{16}O_{38}Zn_3$ $[M^+ + H]^+$: 4232; found: 4232; UV/Vis (THF, 25 °C): λ_{max} (ε) = 415.8 (1 240 000 M^{-1}cm^{-1}), 545.0 nm.

$(3P_{Zn})_4$-ester-P_{FB}: A solution of $[(t\mathrm{BuPh_2Si})_2P_{Zn}]_4$-ester-$P_{FB}$ (14.9 mg, 3 μmol), $1P_{Zn}$ (R = CH_2Br; 44.8 mg, 30 μmol), and anhydrous KF (6.9 mg, 0.12 mmol) in *N*-methylpyrrolidone (1 mL) was heated at 80 °C under Ar for 1 week in the dark. The reaction mixture was then treated in a manner similar to that for the preparation of $(1P_{zn})_1P_{FB}$ to give $(3P_{Zn})_4$-ester-P_{FB} as a red powder in 16 % yield (7 mg). The ^{1}H NMR spectrum was rather broad, even at an elevated temperature, such as 55 °C. This was possibly caused by a much slower conformational change than the NMR timescale. ^{1}H NMR (270 MHz, $CDCl_3$, 55 °C): $\delta = -2.85$ (s, 2H; NH), 3.31 (s, 192H; dendron-Ar$(OCH_3)_2$), 4.50 (s, 64H; outer dendron-CH_2O), 4.88 (s, 32H; inner dendron-CH_2O), 5.14 (s, 24H; CH_2O between P_{Zn} units, between P_{Zn} and P_{FB}), 5.89 (s, 32H; *p*-H in outer dendron-C_6H_3), 6.07 (s, 64H; *o*-H in outer dendron-C_6H_3), 6.25 (s, 16H; *p*-H in inner dendron-C_6H_3), 6.44 (s, 32H; *o*-H in inner dendron-C_6H_3), 6.86 (s, 8H; *p*-H in outer P_{Zn}-C_6H_3), 7.38 (s, 16H; *o*-H in outer P_{Zn}-C_6H_3), 7.48 – 7.87 (d, 64H; *o*-H and *m*-H in P_{Zn}-C_6H_4, P_{FB}-C_6H_4), 8.72 – 8.96 (m, 104H; pyrrole-*β*-H in P_{Zn}, P_{FB}), 9.54 ppm (s, 24H; *meso*-H in P_{Zn}); MALDI-TOF MS: calcd for $C_{844}H_{687}N_{52}O_{128}Zn_{12}$ $[M^+ + H]^+$: 14386; found: 14390; UV/Vis (THF, 25 °C): λ_{max} (ε) = 416.1 (2 657 000 M^{-1}cm^{-1}), 544.9 nm.

[1] a) M. R. Wasielewski, *Chem. Rev.* **1992**, *92*, 435 and references therein; b) D. Gust, T. A. Moore in *The Porphyrin Handbook*, *Vol. 8* (Eds.: K. Kadish, K. M. Smith, R. Guilard), Academic Press, New York, **1999**, Chapter 57, p. 153 and references therein.

[2] J. Deisenhofer, H. Michel, *Science* **1989**, *245*, 1463.

[3] a) J. L. Sessler, B. Wang, A. Harriman, *J. Am. Chem. Soc.* **1995**, *117*, 704; b) N. Nagata, S. Kugimiya, Y. Kobuke, *Chem. Commun.* **2000**, 1389.

[4] a) C. A. Hunter, R. K. Hyde, *Angew. Chem.* **1996**, *108*, 2064; *Angew. Chem. Int. Ed. Engl.* **1996**, *35*, 1936; b) A. Prodi, M. T. Indelli, C. J. Kleverlaan, F. Scandola, E. Alessio, T. Gianferrara, L. G. Marzilli, *Chem. Eur. J.* **1999**, *5*, 2668; c) R. A. Haycock, A. Yartsev, U. Michelsen, V. Sundström, C. A. Hunter, *Angew. Chem.* **2000**, *112*, 3762; *Angew. Chem. Int. Ed.* **2000**, *39*, 3616; d) Y. Kudora, K. Sugou, K. Sasaki, *J. Am. Chem. Soc.* **2000**, *122*, 7833.

[5] a) S. Prathapan, T. E. Johnson, J. S. Lindsey, *J. Am. Chem. Soc.* **1993**, *115*, 7519; b) A. Nakano, A. Osuka, I. Yamazaki, T. Yamazaki, Y. Nishimura, *Angew. Chem.* **1998**, *110*, 3172; *Angew. Chem. Int. Ed.* **1998**, *37*, 3023; c) J. Li, A. Ambroise, S. I. Yang, J. R. Diers, J. Seth, C. R. Wack, D. F. Bocian, D. Holten, J. S. Lindsey, *J. Am. Chem. Soc.* **1999**, *121*, 8927.

[6] a) V. S.-Y. Lin, S. G. DiMagno, M. J. Therien, *Science* **1994**, *264*, 1105; b) R. W. Wagner, T. E. Johnson, J. S. Lindsey, *J. Am. Chem. Soc.* **1996**, *118*, 11166.

[7] D. Gust, *Nature* **1997**, *386*, 21.

[8] a) M. G. H. Vicente, L. Japuinod, K. M. Smith, *Chem. Commun.* **1999**, 1771; b) H. L. Anderson, *Chem. Commun.* **1999**, 2323; c) A. K. Burrell, D. L. Officer, P. G. Plieger, D. C. W. Reid, *Chem. Rev.* **2001**, *101*, 2751 and references therein.

[9] G. McDermott, S. M. Prince, A. A. Freer, A. M. Hawtornthwaite-Lawless, M. Z. Papiz, R. J. Cogdell, N. W. Isaacs, *Nature* **1995**, *374*, 517.

[10] a) G. M. Stewart, M. A. Fox, *J. Am. Chem. Soc.* **1996**, *118*, 4354; b) C. Devadoss, P. Bharathi, J. S. Moore, *J. Am. Chem. Soc.* **1996**, *118*, 9635; c) D.-L. Jiang, T. Aida, *Nature* **1997**, *388*, 454; d) D.-L. Jiang, T. Aida, *J. Am. Chem. Soc.* **1998**, *120*, 10895; e) T. Sato, D.-L. Jiang, T. Aida, *J. Am. Chem. Soc.* **1999**, *121*, 10658; f) S. L. Gilat, A. Andronov, J. M. J. Fréchet, *Angew. Chem.* **1999**, *111*, 1519; *Angew. Chem. Int. Ed.* **1999**, *38*, 1422; g) Y. Wakabayashi, M. Tokeshi, A. Hibara, D.-L. Jiang, T. Aida, T. Kitamori, *J. Phys. Chem. B* **2001**, *105*, 4441; h) M. Maus, R. De, M. Lor, T. Weil, S. Mitra, U.-M. Wiesler, A. Herrmann, J. Hofkens, T. Vosch, K. Müllen, F. C. De Schryver, *J. Am. Chem. Soc.* **2001**, *123*, 7668.

[11] a) A. Bar-Haim, J. Klafter, R. Kopelman, *J. Am. Chem. Soc.* **1997**, *119*, 6197; b) A. Bar-Haim, J. Klafter, *J. Phys. Chem. B* **1998**, *102*, 1662; c) S. Tretiak, V. Chernyak, S. Mukamel, *J. Phys. Chem. B* **1998**, *102*, 3310.

[12] a) D. L. Officer, A. K. Burrell, D. C. W. Reid, *Chem. Commun.* **1996**, 1657; b) C. C. Mak, N. Bampos, J. K. M. Sanders, *Angew. Chem.* **1998**, *110*, 3169; *Angew. Chem. Int. Ed.* **1998**, *37*, 3020; c) C. C. Mak, D. Pomeranc, M. Montalti, L. Prodi, J. K. M. Sanders, *Chem. Commun.* **1999**, 1085; d) K.-I. Sugiura, H. Tanaka, T. Matsumoto, T. Kawai, Y. Sakata, *Chem. Lett.* **1999**, 1193; e) N. Maruo, M. Uchiyama, T. Kato, T. Arai, H. Akisada, N. Nishino, *Chem. Commun.* **1999**, 2057; f) E. K. L. Yeow, K. P. Ghiggino, J. N. H. Reek, M. J. Crossley, A. W. Bosman, A. P. H. J. Schenning, E. W. Meijer, *J. Phys. Chem. B* **2000**, *104*, 2596.

[13] M.-S. Choi, T. Aida, T. Yamazaki, I. Yamazaki, *Angew. Chem.* **2001**, *113*, 3294; *Angew. Chem. Int. Ed.* **2001**, *40*, 3194.

[14] G. L'abbé, B. Forier, W. Dehaen, *Chem. Commun.* **1996**, 2143.

[15] See the Supporting Information.

[16] J.-S. Hsiao, B. P. Krueger, R. W. Wagner, T. E. Johnson, J. K. Delaney, D. C. Mauzerall, G. R. Fleming, J. S. Lindsey, D. F. Bocian, R. J. Donohoe, *J. Am. Chem. Soc.* **1996**, *118*, 11181.

[17] R. L. Brookfield, H. Ellul, A. Harriman, G. Porter, *J. Chem. Soc. Faraday Trans. 2*, **1986**, *82*, 219.

[18] a) T. Förster, *Z. Naturforsch.* **1949**, *4a*, 321; b) T. Förster, *Discuss. Faraday. Soc.* **1959**, *27*, 7.

Received: December 17, 2001 [F3742]

  0947-6539/02/0812-2678 $ 20.00+.50/0